COBEM 2023 27TH INTERNATIONAL CONGRESS OF MECHANICAL ENGENEERING

ABCM Brazilian Society of Mechanical Sciences and Engineering
27th ABCM International Congress of Mechanical Engineering
December 04-08, 2023, Florianópolis-SC, Brazil

COB-2023-2065
NUMERICAL SIMULATION OF A TURBULENT JET DIFFUSION FLAME OF DIMETHYL ETHER USING LES

Jonatan Ismael Eisermann
Federal University of Rio Grande do Sul (UFRGS) - Graduate Program in Applied Mathematics (PPGMAp), Av. Bento Gonçalves, 9500 - Agronomia, Porto Alegre - RS, 91509-900, Brazil
jonatan.eisermann@ufrgs.br

Álvaro Luiz de Bortoli
Federal University of Rio Grande do Sul (UFRGS) - Graduate Program in Applied Mathematics (PPGMAp) and Graduate Program in Chemical Engineering (PPGEQ), Av. Bento Gonçalves, 9500 - Agronomia, Porto Alegre - RS, 91509-900, Brazil
dbortoli@mat.ufrgs.br

Abstract. *The objective of the present work is to obtain numerical solutions for a turbulent jet diffusion flame of dimethyl ether (DME) in a burner. Thus, a mathematical model based on the combustion process is formulated and solved on a three-dimensional computational mesh of the burner geometry. Under the assumption of low Mach number flow, equations that model a jet diffusion flame include those for the continuity, momentum, mixture fraction, enthalpy/temperature and concentration of the chemical species, which generate a system of partial differential equations highly nonlinear and often difficult to solve. After generating the computational mesh, the fourth-order Finite Difference method is used for Large-Eddy Simulation (LES), with the Smagorinsky model for turbulent viscosity. Using LES, structures larger than the size of the computational mesh are computed explicitly, while small-scale effects are modeled. The resulting algebraic system for the flow is then solved by the Simplified Runge-Kutta method. The chemical part of the flame is modeled by a three-step DME combustion model, with Arrhenius coefficients, and integrated using Rosenbrock's semi-implicit method. For validation purposes, the numerical results obtained are compared with experimental data from the Sandia National Laboratories and show good agreement. Furthermore, these results help in understanding concepts related to mixing, reaction and combustion of turbulent jet diffusion flames of dimethyl ether that are not yet fully understood.*

Keywords: *DME jet diffusion flame, Large-Eddy Simulation, Finite Difference, Simplified Runge-Kutta, Rosenbrock.*

1. INTRODUCTION

Dimethyl ether (DME) is the simplest ether, a fuel whose chemical structure consists of two methyl groups bonded to an oxygen atom, expressed by the chemical formula CH_3OCH_3. Its production occurs mainly from natural gas, coal and biomass, a factor that makes it a (bio)fuel with high production availability. Despite being a gaseous fuel under normal conditions, it can be easily liquefied (at 0.6 MPa) and can replace diesel through few engine modifications (Wang *et al.*, 2000; Jie *et al.*, 2010). Compared to traditional petroleum fuels such as liquefied petroleum gas and diesel, DME is a high-efficiency compression-ignition fuel with absence of any bond between carbon atoms and, therefore, with reduced emissions of soot. These characteristics make it a good alternative fuel and, consequently, increase the relevance of studies on its combustion.

For validation purposes, in 2010, the International Workshop on Measurement and Computation of Turbulent Non-premixed Flames (TNF Workshop, 2010) defined a new series of benchmark flames consisting of partially premixed piloted DME/air jet flames. This series of five turbulent jet flames (Sandia DME D, E, F, G and G') into a co-flow of air spans jet exit Reynolds numbers from approximately $29,300$ to $73,250$ and, as the well-known Sandia piloted methane/air jet flames (Barlow and Frank, 2003), are stabilized on the Sydney piloted burner. Despite the similarity of burner geometry, in the Sandia DME flames the intensity of turbulence–chemistry interactions is lower than in the Sandia methane flames, for the same Reynolds number, and fewer extinction events are observed. So, higher Reynolds numbers are needed for DME flames when compared to corresponding methane flames to observe significant effects of turbulence on the flame structure (Neuber *et al.*, 2019).

Overall, for both methane and DME, the Sandia flames D-F form important fields of study for turbulent combustion modellers as they exhibit turbulence–chemistry interactions increasing from relatively low levels in flame D through to strong interactions and near blow-off conditions in flame F (Neuber *et al.*, 2019). Specifically for Sandia DME D, Coriton *et al.* (2015) published velocity and laser-induced fluorescence data for hydroxyl (OH) and formaldehyde (CH_2O), while Fuest *et al.* (2015) present 1D Raman/Rayleigh measurements of seven major species (CO_2, O_2, CO, N_2, DME, H_2O, H_2) and temperature. The comparison with the corresponding piloted methane flame showed differences in these

two jet flames, attributed to differences in fuel consumption rates and product species formation in the fuel-rich region. Furthermore, it was observed that extinction events are less frequent when DME is used as fuel.

The reported differences between methane and DME flames, the availability of a large set of experimental data and the relevance of DME fuel nowadays are the motivations for this work. Here, the purpose is the investigation of the turbulent structure of the Sandia DME D flame using Large-Eddy Simulation (LES) with the Smagorinsky model for turbulent viscosity (Smagorinsky, 1963). In the LES methodology, structures larger than the size of the used computational mesh are considered as the eddies that contain greater amounts of energy and so are computed explicitly; while the small scales, which have a more universal behavior, are implicitly approximated by sub-grid models. Therefore, the computational cost of the LES method is usually lower than direct numerical simulation techniques, such as the classic Direct Numerical Simulation (Peters, 2006).

In order to organize the proposed text and achieve the research objective, this article is structured into three sections in addition to the Introduction. The first section introduces a three-dimensional mathematical model of the phenomenon under consideration based on the equations of continuity, momentum, mixture fraction, temperature and concentration of the five major chemical species. Moreover, it provides details related to the solution procedure, including the computational mesh, discretization technique and resolution method used for the mathematical model. The second section presents the numerical results obtained for the turbulent Sandia DME D flame, comparing them with experimental data from the Sandia National Laboratories at four axial positions and one radial position. This allows for an analysis of the flame's composition across the entire spatial domain. Finally, the last section offers insights into the computational simulation conducted, encompassing an evaluation of the numerical methods employed to solve the model equations and providing suggestions for future research.

2. METHODOLOGY

Piloted turbulent DME/air jet flames, as introduced previously in TNF Workshop (2010), were investigated on the burner configuration of the Sydney/Sandia piloted flame series. Through three coaxial jets, this burner generates a diffusive flame in which the fuel is injected from a central tube with diameter $d = 7.45$ mm, and a pilot annulus with inner and outer diameter of 8 mm and 18.2 mm, respectively, is used to stabilize the flame. To enable combustion, a co-flow of air, at ambient conditions, of 25.4 cm $\times$ 25.4 cm is injected and surrounds the pilot jet, as shown in Fig. 1.

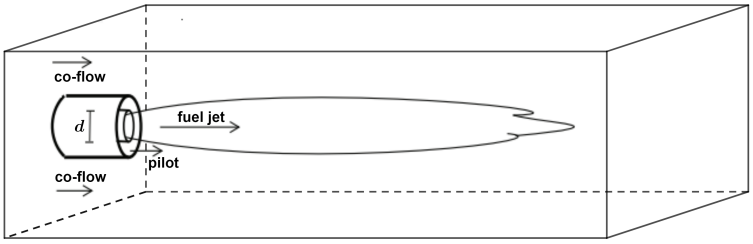

Figure 1. Sydney piloted burner sketch.

The bulk velocities for the main jet, the pilot and the co-flow exit are respectively 45.9 m/s, 1.1 m/s and 0.9 m/s. Furthermore, the unburnt gas compositions of the Sandia DME D flame are presented in Table 1.

Table 1. Unburnt gas compositions (in mole fractions) of the jet, pilot, and co-flow streams of Sandia DME D flame.

	CH_3OCH_3	C_2H_2	H_2	N_2	O_2	Ar	H_2O	CO_2
Jet	0.2	—	—	0.6237	0.1673	0.0075	0.0008	0.0003
Pilot	—	0.0218	0.0878	0.6793	0.1718	0.0077	0.0012	0.0303
Co-flow	—	—	—-	0.7746	0.2078	0.0093	0.008	0.0004

Pilot flows of C_2H_2, H_2, N_2, air and CO_2 are selected to match the product composition and temperature of a premixed DME–air flame at 0.6 equivalence ratio, but with higher flame speed (Fuest *et al.*, 2015). The 20% DME and 80% air composition of the fuel injected into the burner provides the jet kinematic viscosity $\nu_1 = 1.167 \cdot 10^{-5}$ m^2/s and the stoichiometric value of the mixture fraction $Z_{st} = 0.35$. These quantities are present in the equations that model the studied flame, as we will see in the next subsection.

2.1 Model Formulation

The mathematical model of the Sandia DME D flame done in this work is based on the assumptions that inside the burner the flow has a low Mach-number, the pressure remains almost constant, the heat losses through the walls are small

and the contribution due to the radiation is negligible — weak hypotheses, as they usually happen inside a burner (Peters, 2006). The equations that constitute the model are the equation of continuity, momentum (Navier-Stokes equations), mixture fraction, temperature and chemical species concentration. These equations, in a primary formulation, involve dependent variables on the space $\mathbf{x} = (x_1, x_2, x_3)$ and on the time t: the density ρ; the velocity vector $\mathbf{u} = (u_1, u_2, u_3)$, where the component u_i corresponds to the velocity of the fluid along the x_i-direction, $i = 1, 2, 3$; the pressure p; the temperature T; and the species molar concentration $[\mathcal{S}]$, for each chemical specie (here denoted generically by $\mathcal{S}$) considered in the combustion.

In LES, Favre averaging or density-weighted averaging method is commonly used in compressible flow to separate turbulent fluctuations from the mean-flow. This filtering results a simplistic form for the nonlinear convective terms of the Navier-Stokes equations when compared to Reynolds averaging (De Bortoli, 2009). In Favre decomposition, except for density and pressure, every dependent variable Φ involved in the governing equations is written as a sum between an average component $\tilde{\Phi}$ and a fluctuation $\Phi^{''}$. So, we put

$$\Phi = \tilde{\Phi} + \Phi^{''}, \qquad \overline{\rho\Phi^{''}} = 0,$$

where $\bar{(\cdot)}$ denotes the Reynolds averaging (Peters, 2006).

Together with a nondimensionalization procedure and the Boussinesq hypothesis to model the Reynolds stress tensor, the application of the Favre decomposition on the set of governing equations results in the following equations (De Bortoli *et al.*, 2015):

- Momentum

  Using Einstein notation for a compressible fluid, the equation of momentum that also satisfies the equation of continuity is

  $$\frac{\partial(\bar{\rho}\bar{u}_i)}{\partial t} + \frac{\partial(\bar{\rho}\bar{u}_i\bar{u}_j)}{\partial x_j} = \frac{-1}{M^2}\frac{\partial \bar{p}}{\partial x_i} + \frac{\partial}{\partial x_j}\left(\frac{1}{R}\bar{\sigma}_{ij}\right), \tag{1}$$

  where M is the Mach number, which compare the speed of the fluid with the speed of sound; R is the Reynolds number, which determines the fluid flow regime; and

  - $\bar{\sigma}_{ij} = \bar{\mu}_t(2\tilde{S}_{ij} - \frac{2}{3}\delta_{ij}\tilde{S}_{kk})$ is the viscous stress tensor;
  - δ_{ij} is the Kronecker Delta: $\delta_{ij} = \begin{cases} 1, & \text{if } i = j \\ 0, & \text{otherwise} \end{cases}$;
  - $\tilde{S}_{ij} = \frac{1}{2}\left(\frac{\partial \tilde{u}_i}{\partial x_j} + \frac{\partial \tilde{u}_j}{\partial x_i}\right)$ is the rate of strain tensor;
  - $\bar{\mu}_t = \bar{\rho}(C\Delta)^2|\tilde{S}_{ij}|$ is the turbulent viscosity.

  Here, we employ the Large-Eddy Simulation technique with the Smagorinsky model for $\bar{\mu}_t$. So, C is the Smagorinsky coefficient, $\Delta = (\mathrm{d}x_1\,\mathrm{d}x_2\,\mathrm{d}x_3)^{1/3}$ is the mesh filter size and $|\cdot|$ denotes the Frobenius norm. Our choice for the coefficient was $C = 0.09$.

- Mixture fraction

  In a system with two feeders like a diffusion flame, where a fuel mass flow m_1 is mixed with an oxidant stream of mass flow m_2, the mixture fraction Z measures the mixture of reagents and is given by the ratio

  $$Z = \frac{m_1}{m_1 + m_2}.$$

  On our study, the equation of mixture fraction on space and time is given by

  $$\frac{\partial(\bar{\rho}\bar{Z})}{\partial t} + \frac{\partial(\bar{\rho}\tilde{u}_j\tilde{Z})}{\partial x_j} = \frac{\partial}{\partial x_j}\left(\frac{\bar{\mu}_t}{RS}\frac{\partial \tilde{Z}}{\partial x_j}\right), \tag{2}$$

  where S is the Schmidt number, which relates the viscosity and the mass diffusivity of the fluid.

- Temperature

  The Burke-Schumann solution for diffusion flames provides an analytical formulation for temperature T as a function of mixture fraction Z. Based on this approach, for a hydrocarbon or alcohol fuel, F, of global combustion reaction

  $$\nu_F\mathrm{F} + \nu_{\mathrm{O}_2}\mathrm{O}_2 \rightarrow \nu_{\mathrm{CO}_2}\mathrm{CO}_2 + \nu_{\mathrm{H}_2\mathrm{O}}\mathrm{H}_2\mathrm{O},$$

where $\nu_{\mathcal{S}}$ denotes the stoichiometric coefficient of the chemical species $\mathcal{S}$, we consider the following equation for unburnt and burnt gas temperature (T_u and T_b, respectively):

$$T_u(Z) = T_2 + (T_1 - T_2)Z, \tag{3}$$

$$T_b(Z) = \begin{cases} T_u + \left(\frac{QY_{\mathrm{F},1}}{c_p \nu_{\mathrm{F}} \mathrm{W_F}}\right) Z, & \text{if } Z \leq Z_{st} \\ T_u + \left(\frac{QY_{\mathrm{O_2},2}}{c_p \nu_{\mathrm{O_2}} \mathrm{W_{O_2}}}\right)(1-Z), & \text{otherwise} \end{cases}, \tag{4}$$

where

- T_1 and $Y_{\mathrm{F},1}$ are, respectively, the temperature and the fuel mass fraction in the fuel stream;
- T_2 and $Y_{\mathrm{O_2},2}$ are, respectively, the temperature and the O_2 mass fraction in the oxidant stream;
- Q and c_p are, respectively, the heat of combustion and the specific heat capacities;
- $\mathrm{W_F}$ and $\mathrm{W_{O_2}}$ denote, respectively, the molecular weight of the fuel and of $\mathrm{O_2}$;
- Z_{st} is the stoichiometric value of the mixture fraction.

- Chemical species concentration

  Modeling complete chemical kinetics of a DME-air diffusion flame involves a large number of chemical species and reactions. This can be extremely computationally intensive. Thus, in an effort to reduce the computational burden and simplify the numerical result corresponding to the concentration of chemical species, we have developed a simplified mechanism consisting of the global three-step reactions presented in Table 2, along with their associated Arrhenius parameters.

Table 2. DME-air three-step chemical reactions with Arrhenius coefficients

i	i-th reaction	Pre-exponential factor A_i [mol/(m$^3\cdot$ s)]	Activation energy E_i [J/mol]
1	$\mathrm{CH_3OCH_3 + 2\,O_2 \xrightarrow{k_1} 2\,CO + 3\,H_2O}$	$8.93 \cdot 10^5$	120,685
2	$\mathrm{CO + 0.5\,O_2 \xrightarrow{k_2} CO_2}$	$1.07 \cdot 10^{-1}$	-44,257
3	$\mathrm{CO_2 \xrightarrow{k_3} CO + 0.5\,O_2}$	$6.23 \cdot 10^{-8}$	-201,758

From this sequence of net reactions, the set of equations for the concentration of the five major species ($\mathrm{CO_2}$, $\mathrm{O_2}$, CO, $\mathrm{CH_3OCH_3}$, $\mathrm{H_2O}$) becomes

$$\begin{cases} \frac{\partial}{\partial t}[\mathrm{CH_3OCH_3}] &= -k_1[\mathrm{CH_3OCH_3}][\mathrm{O_2}]^2 \\ \frac{\partial}{\partial t}[\mathrm{O_2}] &= -2k_1[\mathrm{CH_3OCH_3}][\mathrm{O_2}]^2 - 0.5k_2[\mathrm{CO}][\mathrm{O_2}]^{0.5} + 0.5k_3[\mathrm{CO_2}] \\ \frac{\partial}{\partial t}[\mathrm{CO}] &= 2k_1[\mathrm{CH_3OCH_3}][\mathrm{O_2}]^2 - k_2[\mathrm{CO}][\mathrm{O_2}]^{0.5} + k_3[\mathrm{CO_2}] \\ \frac{\partial}{\partial t}[\mathrm{H_2O}] &= 3k_1[\mathrm{CH_3OCH_3}][\mathrm{O_2}]^2 \\ \frac{\partial}{\partial t}[\mathrm{CO_2}] &= k_2[\mathrm{CO}][\mathrm{O_2}]^{0.5} - k_3[\mathrm{CO_2}] \end{cases}, \tag{5}$$

where $[\mathcal{S}]$ denotes the molar concentration of $\mathcal{S}$ and, for $i = 1, 2, 3$, we have from Arrhenius equation that

$$k_i(T) = A_i e^{-E_i/(RT)},$$

with the universal gas constant $R = 8.314$ J/(mol·K).

The Eqs. (1)-(5) constitute the mathematical model used to simulate the Sandia DME D flame. We will see in the following subsection the numerical procedures to be used to solve these equations.

2.2 Solution Procedure

The numerical resolution of the mathematical model previously developed requires that we discretize the domain, in order to transform the real solution of the model (a continuous function) into a discrete function defined at each point in space and time. In this context, we consider a computational mesh, Ω, formed by $199 \times 69 \times 69$ points on the x, y and z (x_1, x_2 and x_3) directions, respectively, to cover the burner in Fig. 1 with dimensions $70d \times 7d \times 7d$. So, $\Omega = \{(x_i, y_j, z_k); i = 1, 2, \ldots, 199;\ j = 1, 2, \ldots, 69;\ k = 1, 2, \ldots, 69\}$.

After generating a computational mesh in the domain, initial and boundary conditions corresponding to the flame characteristics are defined on the mesh points. Also, the fourth-order Finite Difference method is used to calculate approximations, at each point, of the derivatives present in the governing equations, as part of the LES methodology with the Smagorinsky model for turbulent viscosity. The resulting algebraic system for the flow is then solved by the Simplified Runge-Kutta method, while the chemical part of the flame is integrated using Rosenbrock's semi-implicit method.

2.2.1 Simplified Runge-Kutta Method

To solve the discretized form of the equations (1) and (2) we use the Simplified Runge-Kutta method with three stages. This method is explicit and characterized by its low computational cost, simplicity of implementation and good levels of robustness (De Bortoli *et al.*, 2015). So, the system

$$\frac{\partial \mathbf{w}}{\partial t} = -\mathbf{r},$$

with $\mathbf{w} = [\bar{\rho}\tilde{u}_1, \bar{\rho}\tilde{u}_2, \bar{\rho}\tilde{u}_3, \bar{\rho}\tilde{Z}]^T$ and $\mathbf{r}$ corresponds to the convective and diffusive terms of the equations (1) and (2), is solved at each point of Ω through an iterative process over time given by

$$\begin{aligned}
\mathbf{w}_{i,j,k}^{(0)} &= \mathbf{w}_{i,j,k}^{(n)} \\
\mathbf{w}_{i,j,k}^{(s)} &= \mathbf{w}_{i,j,k}^{(0)} - \alpha_s \Delta t\, \mathbf{r}_{i,j,k}^{(s-1)}, \qquad s = 1, 2, 3; \\
\mathbf{w}_{i,j,k}^{(n+1)} &= \mathbf{w}_{i,j,k}^{(3)},
\end{aligned}$$

where Δt is the time step, and $\mathbf{w}_{i,j,k}^{(h)}$ and $\mathbf{r}_{i,j,k}^{(h)}$ correspond, respectively, to approximations of the vector $\mathbf{w}$ and the vector $\mathbf{r}$ at the mesh point (x_i, y_j, z_k) at time $h \cdot \Delta t$ seconds. Our choice of coefficients of the method are obtained analytically for a second-order temporal approximation (Butcher, 1987): $\alpha_1 = 0.5$, $\alpha_2 = 0.5$ and $\alpha_3 = 1$.

Runge-Kutta methods are preferred because, for a given time step, the errors produced are usually smaller than those of competing methods (De Bortoli *et al.*, 2015). More specifically, the Simplified Runge-Kutta is an explicit method and, therefore, works well with small time steps — a necessary characteristic to represent the mixture in a turbulent flow. We use the Simplified Runge-Kutta method with time step $\Delta t = 5 \cdot 10^{-6}$ seconds, in order to obtain the numerical solution of the flame, at all points of the computational mesh, until the instant of time 1 second.

It is worth mentioning that the calculation of Z at each point of Ω allows us to obtain the respective temperature value through Eqs. (3)-(4). We use these temperature values to obtain the concentrations of the chemical species, as explained in the following subsection.

2.2.2 Rosenbrock Method

The Rosenbrock method is a semi-implicit method inherent to the Runge-Kutta methods class. At each step the method require the solution of a linear system of equations, simplifying the solution of the problem compared to the implicit Runge-Kutta method. Under the appropriate initial conditions ($\mathbf{c}_0$), we solve the system

$$\frac{\partial \mathbf{c}}{\partial t} = \mathbf{f}, \qquad \mathbf{c} = [c_1, c_2, c_3, c_4, c_5]^T, \tag{6}$$

where $c_1 = [CH_3OCH_3]$, $c_2 = [O_2]$, $c_3 = [CO]$, $c_4 = [H_2O]$, $c_5 = [CO_2]$ and $\mathbf{f}$ corresponds to the right side of the system in Eq. (5), through a fourth-order Rosenbrock method with four stages. So, given a initial time step h_0 and real parameters ω_i, α_{ij}, β, previously chosen according to the desired order of consistency and stability to the method, an iterative process is developed over time in which at each iteration, n, we compute

$$\mathbf{A}_n = \mathbf{I}_5 - h_n \beta \frac{\partial \mathbf{f}}{\partial \mathbf{c}}\bigg|_{\mathbf{c}_n},$$

where $\mathbf{I}_5$ is the Identity matrix of size 5, and calcule the stages $\mathbf{k}_i$, $i = 1, 2, 3, 4$, by

$$\begin{aligned}
\mathbf{k}_1 &= \mathbf{A}_n^{-1}\mathbf{f}\left(\mathbf{c}_n\right); & \mathbf{k}_2 &= \mathbf{A}_n^{-1}\mathbf{f}\left(\mathbf{c}_n + h_n\alpha_{21}\mathbf{k}_1\right); \\
\mathbf{k}_3 &= \mathbf{A}_n^{-1}\mathbf{f}\left(\mathbf{c}_n + h_n(\alpha_{31}\mathbf{k}_1 + \alpha_{32}\mathbf{k}_2)\right); & \mathbf{k}_4 &= \mathbf{A}_n^{-1}\mathbf{f}\left(\mathbf{c}_n + h_n(\alpha_{41}\mathbf{k}_1 + \alpha_{42}\mathbf{k}_2 + \alpha_{43}\mathbf{k}_3)\right).
\end{aligned}$$

Then, we update $\mathbf{c}$ by

$$\mathbf{c}_{n+1} = \mathbf{c}_n + h_n \sum_{i=1}^{4} \omega_i \mathbf{k}_i.$$

Similarly $\mathbf{c}_{n+1}$ was uptaded from $\mathbf{c}_n$ through a time step h_n, we compute $\mathbf{c}_{n+1}^*$ from $\mathbf{c}_n$ using two consecutive iterations with step size $h_n/2$. Then a local estimate of the error, ϵ, is determined by

$$\epsilon = \left\|\mathbf{c}_{n+1} - \mathbf{c}_{n+1}^*\right\|_\infty,$$

where $\|\cdot\|_\infty$ denotes the infinity norm (also called maximum norm). For step size control, if $\epsilon \leq \epsilon_{\max}$ we advance to the next iteration with $\mathbf{c}_{n+1}$ and

$$h_{n+1} = \min\left\{h_{\max}; h_n \min\left[\frac{3}{2}; \max\left(\frac{1}{2}; \frac{9}{10}\left(\frac{\epsilon_{\max}}{\epsilon}\right)^{\frac{1}{5}}\right)\right]\right\}.$$

Otherwise, we advance the iterative process with $\mathbf{c}_{n+1}$ and $h_{n+1} = h_n$.

Our choice of tolerances and parameters are $\epsilon_{\max} = 10^{-10}$, $h_0 = 10^{-5}$, $h_{\max} = 10^7$ and those present in Tab. 3.

Table 3. Parameters for Rosenbrock method.

Parameter	Value	Parameter	Value
α_{21}	-0.5000000000	ω_1	0.9451564786
α_{31}	-0.1012236115	ω_2	0.3413231720
α_{32}	0.9762236115	ω_3	0.5655139575
α_{41}	-0.3922096763	ω_4	-0.8519936081
α_{42}	0.7151140251	β	0.5728160625
α_{43}	0.1430371625		

3. RESULTS AND DISCUSSIONS

The mathematical model and solution procedure described in the previous section have been implemented computationally into a code in Fortran 90. From that code, numerical results for the turbulent Sandia DME D flame were calculated and compared with experimental data from the Sandia National Laboratories at four axial positions ($x/d = 5$, 10, 20 and 40), and in one radial position (at the centerline of the burner) to cover the full composition space of the flame. Here, we consider the axial and radial coordinates to be the x and y coordinates, respectively.

We first compare computed mixture fraction and temperature against the experimental data at the jet centerline, as shown in Fig. 2.

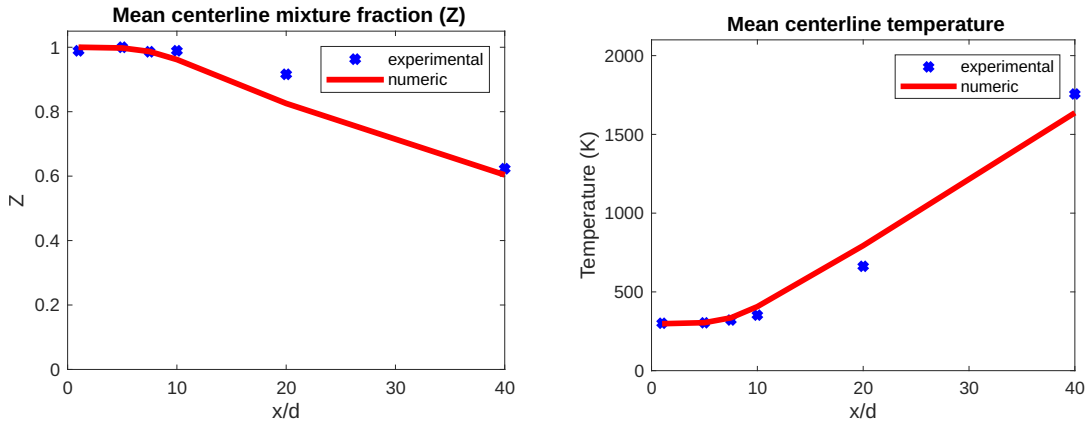

Figure 2. Mixture fraction (left) and temperature (right) at jet centerline.

From the above graphs we can see good levels of agreement between the experimental and numerical data for the mixture fraction. Despite a small discrepancy at $x/d = 20$, the curve of the numerical data is very close to the experimental data in the first two positions and also in the last position analyzed. We also observe that the mixture fraction stay close to 1 for $x/d \leq 10$, which indicates a low level of burning due to little mixing between fuel and oxidant in this region. Consequently, the temperature remains approximately constant and there are no considerable levels of heat release, as shown in the right graph of Fig. 2. After $x/d = 10$, the fuel oxidation begins to occur with greater intensity in the jet centerline, which causes the mixture fraction curve to fall and the temperature curve to rise.

Jet flames structure is complex, because a jet usually starts with a potential zone of 2 to 10 diameters length and ends with a turbulent plume which is very difficult to be simulated by the conventional numerical techniques, including Reynolds Averaged Navier-Stokes (RANS) and LES. Thus, it is natural that, among the axial positions simulated in this work, the greatest discrepancies are concentrated in $x/d = 20$ and $x/d = 40$. We can also observe this analyzing the axial positions, as shown for the mixture fraction in Fig. 3 and for the temperature in Fig. 4.

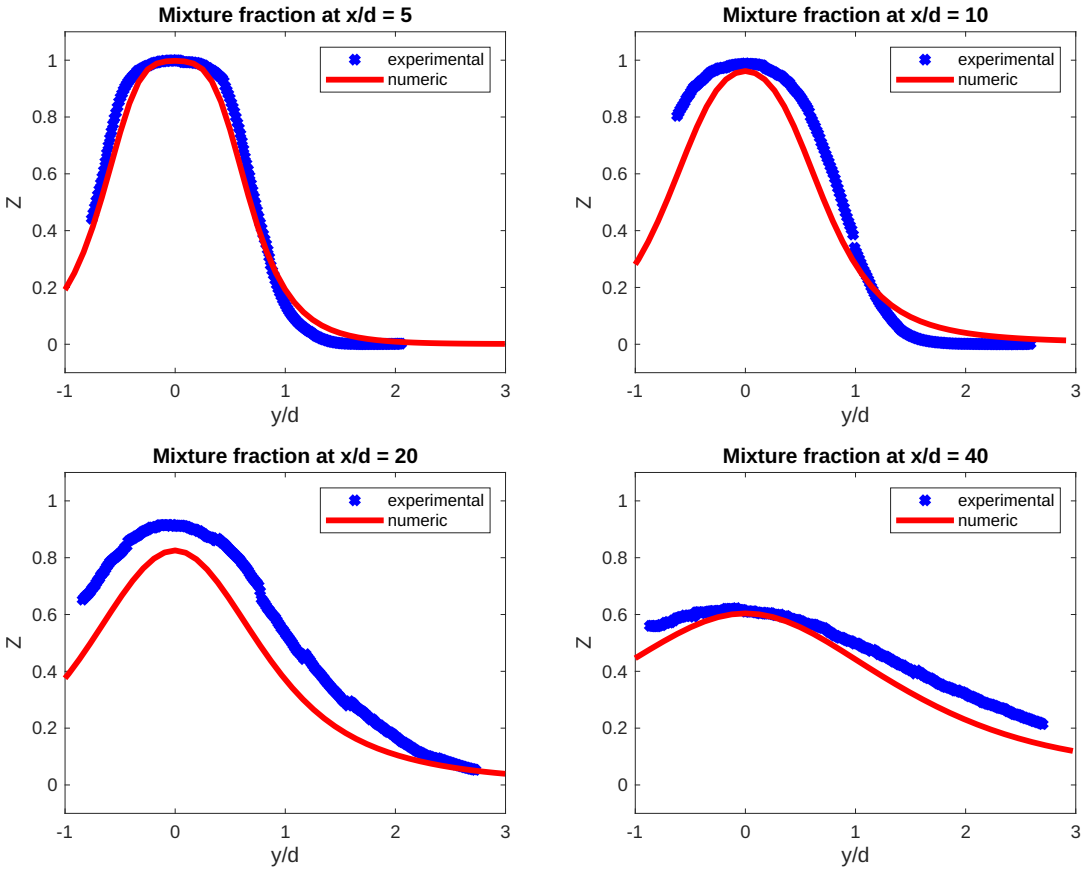

Figure 3. Mixture fraction at axial positions.

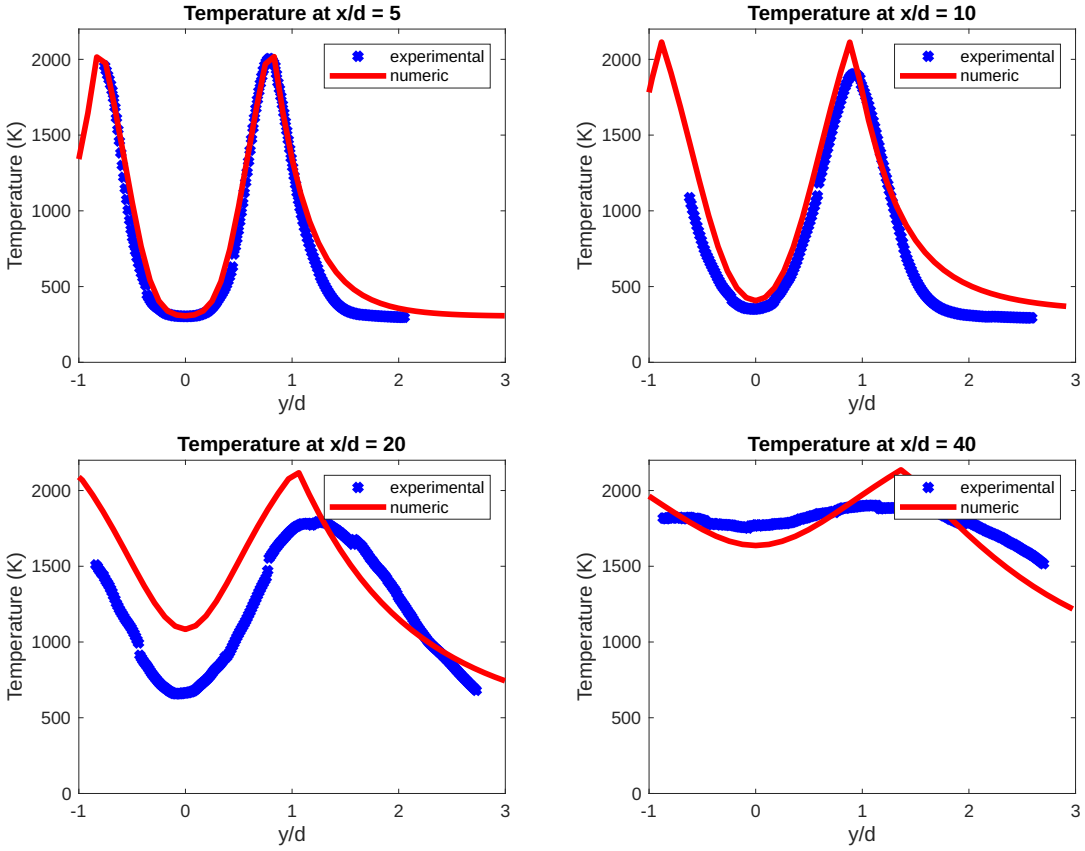

Figure 4. Temperature at axial positions.

In general our numerical simulation captures satisfactorily the radial dependence of the mixture fraction, but indicates some underprediction of mixture fraction in the intermediate and final part of the flame. As well as the mixture fraction, we were able to obtain good results for the temperature in the initial part of the flame. However, for regions of the flame far away from the jet outlet nozzle the results for the temperature were not so good.

Comparison of results between different axial positions showed a trend towards lower strain rates with increasing axial position. So, the amplitude of the mixture fraction and of the value of temperature at axial positions tends to decrease as the flame advances and the mixing between fuel and oxidant increases. However, the same behavior does not occur for all products of combustion, as evidenced by the experimental data and also by our obtained numerical results (Fig. 5 and Fig. 6).

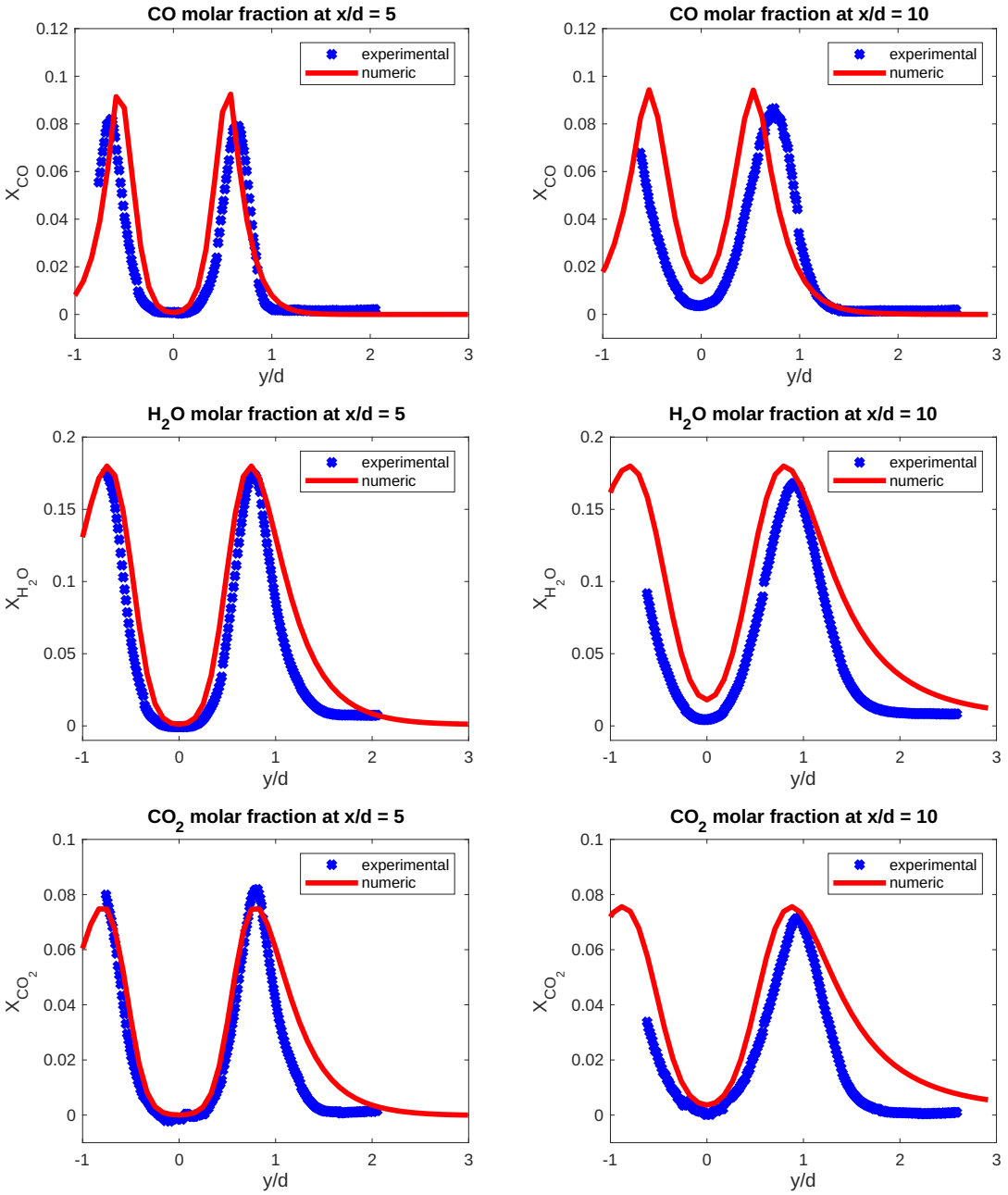

Figure 5. Molar fraction (X) of CO, H_2O and CO_2 at $x/d = 5$ and $x/d = 10$.

Among the products considered in combustion, the CO concentration proved to be the most difficult to be approximate by numerical results. Unlike CO_2 and H_2O production, CO production increases considerably from the jet outlet nozzle to $x/d = 40$, where high temperatures prevail. This because CO is naturally highly sensitive to temperature and has its production peaks at temperatures greater than 1500K.

In general, considering the simplicity of the sequence of net reactions used to model DME combustion, the numerical results for the chemical species were satisfactory. This was mainly due to the effectiveness of the LES methodology

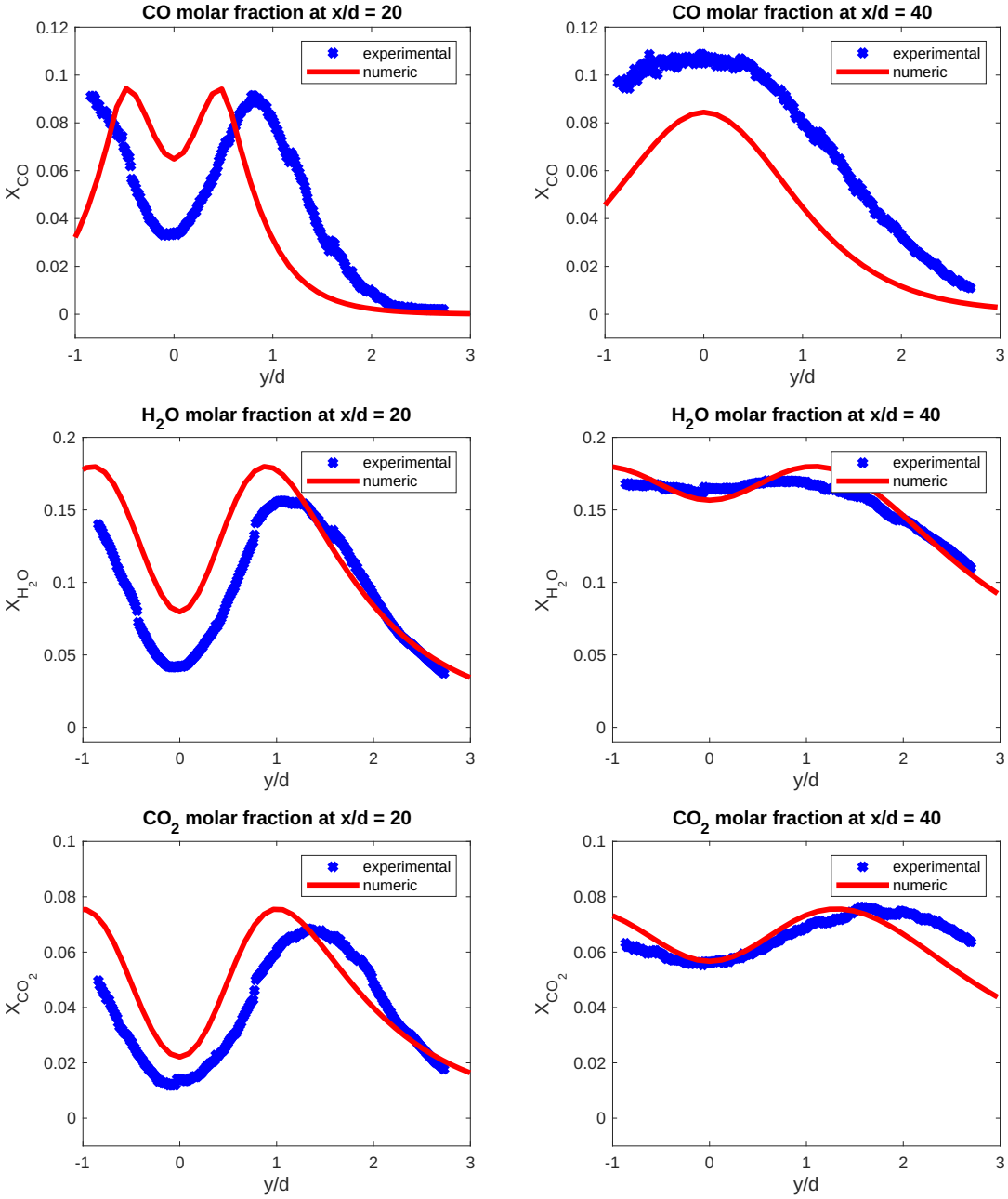

Figure 6. Molar fraction (X) of CO, H_2O and CO_2 at $x/d = 20$ and $x/d = 40$.

combined with the Simplified Runge-Kutta method to solve the flow equations, the reasonable approximations of the temperature by the Burke-Schumann analytical formulation, and the effectiveness of the Rosenbrock method to solve the chemical equations model. Moreover, the judicious choice of our mesh played a crucial role in obtaining satisfactory results. The mesh's high quality was substantiated through a series of simulations where we systematically adjusted mesh resolutions while holding all other parameters constant. Subsequently, we applied GCI (Grid Convergence Index) calculations to the simulation data, allowing us to pinpoint that the selected mesh resolution closely approached the optimal level for achieving accurate and computationally viable results.

4. CONCLUSION

The numerical simulation carried out in this study for the Sandia DME D flame provided important theoretical-practical relationships inherent to combustion. In this sense, the used mathematical model proved to be a representative means of the complex system studied, despite the simplifying assumptions used to calculate the temperature and concentration of chemical species.

Combined with an efficiently method for solving the flow equations, the LES methodology proved to be a viable and

effective means of simulating the flame, since it reduces the computational cost by ignoring the smallest length scales via filtering of the governing equations. Large similarity was found with this technique in mean profiles for axial locations of $x/d \leq 10$. The most significant differences for mixture fraction and temperature remained at $x/d = 20$ and $x/d = 40$, an area of the flame that has a lot of turbulence and is naturally more difficult to simulate.

It is suggested as future works the extension of the present research through the improvement of the mathematical model of the studied flame, mainly through the development of a more detailed kinetic mechanism for the combustion of DME. In addition, numerical comparisons between different methods in the literature can be made, in order to identify a method that is more suitable for solving the model. Also, the study extension for Sandia DME E, F, G and G' flames can be done in order to analyze the consequences of increasing the Reynolds number in the studied system.

5. ACKNOWLEDGEMENTS

We thank the Sandia National Laboratories for providing the experimental data of the piloted DME jet flames. Also, the first author of this work thanks the financial support from the National Council for Scientific and Technological Development (CNPq) - Brazil, under grant number 141504/2021-8. Prof. De Bortoli thanks the CNPq - Brazil under grant number 309271/2021-5.

6. REFERENCES

Barlow, R. and Frank, J., 2003. "Piloted CH4/air flames C, D, E and F - release 2.0." TNF Workshop, https://tnfworkshop.org/data-archives/pilotedjet/ch4-air/. Accessed 02 May 2023.

Butcher, J.C., 1987. *The Numerical Analysis of Ordinary Differential Equations: Runge-Kutta and General Linear Methods*. John Wiley and Sons, New York - USA.

Coriton, B., Zendehdel, M., Ukai, S., Kronenburg, A., Stein, O.T., Im, S.K., Gamba, M. and Frank, J.H., 2015. "Imaging measurements and LES-CMC modeling of a partially-premixed turbulent dimethyl ether/air jet flame". *Proceedings of the Combustion Institute*, Vol. 35, No. 2, p. 1251–1258.

De Bortoli, A.L., 2009. "Analytical/Numerical solution for confined jet diffusion flame (Sandia Flame C)". *Latin American Applied Research*, Vol. 39, No. 1, pp. 157–163.

De Bortoli, A.L., Andreis, G.S.L. and Pereira, F.N., 2015. *Modeling and Simulation of Reactive Flows*. Elsevier, Amsterdam - Netherlands.

Fuest, F., Magnotti, G., Barlow, R.S. and Sutton, J.A., 2015. "Scalar structure of turbulent partially-premixed dimethyl ether/air jet flames". *Proceedings of the Combustion Institute*, Vol. 35, No. 2, p. 1235–1242.

Jie, L., Shenghua, L., Yi, L., Yanju, W., Guangle, L. and Zan, Z., 2010. "Regulated and Nonregulated emissions from a dimethyl ether Powered compression ignition engine". *Energy Fuels*, Vol. 24, No. 4, pp. 2465–2469.

Neuber, G., Fuest, F., Kirchmann, J., Kronenburg, A., Stein, O.T., Galindo-Lopez, S., Cleary, M.J., Barlow, R.S., Coriton, B., Frank, J.H. and Suttond, J.A., 2019. "Sparse-Lagrangian MMC modelling of the Sandia DME flame series". *Combustion and Flame*, Vol. 208, No. 1, pp. 110–121.

Peters, N., 2006. *Turbulent Combustion*. Cambridge University Press, Cambridge - UK.

Smagorinsky, J., 1963. "General circulation experiments with the primitive equations: The basic experiment". *Monthly Weather Review*, Vol. 91, No. 3, pp. 99–164.

TNF Workshop, 2010. "Proceedings of the Tenth International Workshop on Measurement and Computation of Turbulent Nonpremixed Flames". https://tnfworkshop.org/workshop-proceedings/tnf10-workshop/. Accessed 02 May 2023.

Wang, H.W., Zhou, L.B., Jiang, D.M. and Huang, Z.H., 2000. "Study on the performance and emissions of a compression ignition engine fuelled with dimethyl ether". *Journal of Automobile Engineering*, Vol. 214, No. 1, pp. 101–106.

7. RESPONSIBILITY NOTICE

The authors are solely responsible for the printed material included in this paper.